Plasma Deposition of Silicon Nitride Films in a Radial-Flow Reactor

Experimental data on silicon nitride film growth have been obtained from a radial-flow, plasma-enhanced chemical vapor deposition reactor. A nonisothermal mathematical model has been developed consisting of Navier-Stokes, energy, and species balance equations taking into account the temperature dependence of physical properties. The model is predictive at various power input levels for film compositions and growth rates.

Chue-san Yoo
Anthony G. Dixon
Chemical Engineering Department
Worcester Polytechnic Institute
Worcester, MA 01609

Introduction

Silicon nitride thin films have been widely used in microelectronics device fabrication, as diffusion barriers for water vapor and sodium ions, as oxidation masks for selective oxidations, as insulators between metallization layers, and as final passivation layers. The nitride films can be thermally grown in a low-pressure chemical vapor deposition (LPCVD) system with processing temperatures around 700 to 900°C or in a plasma-enhanced chemical vapor deposition (PECVD) reactor at temperatures about 250 to 350°C. Stoichiometric films are deposited in a LPCVD reactor while nonstoichiometric films are formed in a PECVD reactor. Although both processes can produce films of satisfactory quality, there are some circumstances where LPCVD may not be appropriate due to its high processing temperature. For example, in the formation of silicon nitride insulation and passivation layers on GaAs devices and aluminum or gold metallizations, the operating temperature of LPCVD may be destructive to the underlying components. PECVD plays an important role in such cases, as it enables a usually high-temperature reaction to occur at low ambient temperature, through the action of energetic electrons.

The first successful synthesis of a silicon nitride film was reported by Sterling and Swann (1965). The reactant gas mixture could be SiH_4/N_2, SiH_4/NH_3, or $SiH_4/NH_3/N_2$. Generally, if SiH_4/N_2 is used, the silane to nitrogen ratio has to be kept low if a stoichiometric film is desired. The low silane to nitrogen ratio results in low deposition rates. On the other hand, the use of SiH_4/NH_3 seems to be more controllable, resulting in better film thickness and refractive index uniformity (Nguyen et al., 1984) but with higher hydrogen content. The high hydrogen content would affect the film etch rate, stress, and permeability. As a compromise, the reactant gas $SiH_4/N_2/NH_3$ is often used for commercial production.

A PECVD system has a large number of process variables, including power input, pressure, gas flow rate and composition, RF frequency, susceptor temperature, and reactor geometry (Mort and Jansen, 1985). Extensive work has been done, most of which is experimental in nature (Kember et al., 1985; Rosler et al., 1976). It has been well documented that in a PECVD silicon nitride film growth system, it is important not only to have control of the growth rate but also the composition (Samuelson and Mar., 1982). The film Si/N (silicon to nitrogen) atomic ratio is related to its physical properties such as mechanical stress, density, thermal expansion coefficient, resistivity, and breakdown strength. With the large number of variables in the PECVD Si-N-H film growth system, the formulation of a reactor model that can correlate reactor operating conditions to film compositions and growth rates is a necessary approach to understanding and better control of the system.

In this work, a nonisothermal model is presented in which important parameters, such as mean electron energy and density, are obtained from fitting theoretical predictions to experimental data. From this it is possible to show how the values of these two parameters change as operating conditions vary. The predictive nature of the model is then explored by estimating the relevant parameters at one set of conditions, and using them to predict film growth rates and compositions at other conditions.

Experimental Details

The reactor used for the current work was the Applied Materials Plasma II reactor. A gas mixture of $SiH_4/NH_3/N_2$ was used as reactant gas. A diagram of the reactor is shown in Figure 1. The electrodes had a radius of 31.7 cm and a spacing of 5.8 cm. Reactants were fed through a center tube, and flowed

Correspondence concerning this paper should be addressed to A. G. Dixon.
Chue-san Yoo is presently with Taiwan Semiconductor Manufacturing Co. Ltd., 1F, No. 9, Industrial E. 4th Rd., Science-Based Industrial Park, Hsing-chu, Taiwan, Republic of China.

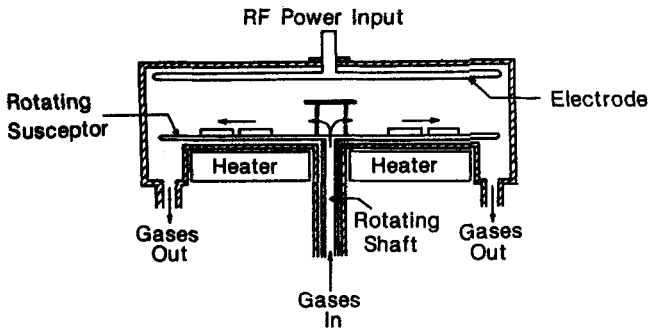

Figure 1. The processing chamber.

centrifugally over the susceptor, on which wafers were placed. The inlet gas shield, made of a flanged quartz base ring with three quartz legs, and an aluminum disk on the top, served to distribute the gas flow uniformly. The top electrode provided the RF power input; the bottom electrode was made of anodized aluminum.

To measure the variation of film growth rates and compositions along the reactor radius, nine silicon substrate wafers (2.54 × 7.62 cm) were placed along the radius. The wafers, which had ⟨111⟩ orientation, were pre-etched with concentrated HF (semiconductor grade low mobile ions), then were rinsed and dried before use. Each run took 50 min of deposition. During this time the silicon nitride was deposited on both the wafers and the bare susceptor. The presence of the wafers did not affect the deposition, and they simply served to allow samples to be taken out of the reactor and analyzed elsewhere. For each run, film thickness and refractive index were measured with an ellipsometer and a film thickness gauge. The ellipsometer used a helium-neon laser having wavelength of 6,328 Å. On each silicon wafer, three points at the same radial position were taken for refractive index and thickness measurements. Weight gain was also measured for each wafer.

The film silicon to nitrogen atomic ratios were derived from the Lorentz-Lorenz correlation (Hill et al., 1969). Sinha and Lugujjo (1978) performed a wide range of experiments on hydrogen-containing silicon nitride films, varying the film Si/N ratio from 0.8 to 1.6, film density from 2.2 to 2.8 g/cm^3, and refractive index from 1.5 to 2.35. Using data fitting, they concluded that the apparent polarizability of silicon can be expressed as $\alpha_{Si} = (1.67 + 1.39\ [Si/N]) \times 10^{-24}$ while $\alpha_N = 0.35 \times 10^{-24}$. The increase of α_{Si} with the Si/N ratio was attributed to the increase of a Si-H complex in the films. Therefore, the average polarizability, α_e, can be expressed as a function of Si/N. So if film refractive index and density are known, one can use the Lorentz-Lorenz correlation

$$\frac{n^2-1}{n^2+2}\frac{M}{\rho} = \frac{4\pi}{3}A\alpha_e \tag{1}$$

to solve for the α_e; and hence the Si/N ratio can be obtained. Since the measured density was the bulk average density of the film on each wafer, the ensuing Lorentz-Lorenz correlation also gave the bulk average Si/N ratio. The Lorentz-Lorenz correlation for calculating the film composition has been used by Reinberg (1979). Bohn and Manz (1985) also indicated that their results were consistent with the correlation.

The third element incorporated in the film was hydrogen, which ranged from 10 to 30 atoms %, but which composed a very small percentage (<2%) by weight. A sophisticated method has been developed by Lanford and Rand (1978) for detecting hydrogen content in the films. For current purposes, the percent hydrogen was estimated by applying additive theory to partial molar volumes of Si, N, and H, which were evaluated from the data of Bohn and Manz. This way of estimating hydrogen content would have negligible effect on the modeling and parameter estimation since the hydrogen weight percentage was very small in the films. The existence of oxygen, possibly resulting from organic compounds back-diffusing from vacuum pumps, may have affected the optical measurement of the films. Our energy-dispersive X-ray (EDX) spectra showed there was a negligible amount of oxygen contained in the films (<1%).

Radial-flow PECVD Reactor Model

A detailed model for a plasma-enhanced chemical vapor deposition reactor should include transport equations for all existing species, neutrals and charged, generated through various ionization and dissociation pathways. The energy balance should not only account for heat transfer due to the heated susceptor but also from the interactions between the gas bulk and the electrical field. The overall model could be very complicated. The current understanding of the chemistry and physics in a glow discharge system does not appear to enable one to formulate a detailed PECVD reactor model as pictured above. The current model is based on the following simplifying assumptions:

1. The amount of charged species is negligible, compared to neutrals
2. Heat generated through the action of the electrical field is negligible, compared to heating from the heated susceptor
3. Incorporation of ions resulting from ion bombardment in the deposited films is negligible

Based on these assumptions, the continuity, momentum, and energy equations can be written:

$$\nabla \cdot (\rho v) = 0 \tag{2}$$

$$\nabla \cdot (\rho v v) = -\nabla P - [\nabla \cdot \tau] + \rho g \tag{3}$$

$$\nabla \cdot (\rho v c_p T) = \nabla \cdot (K \nabla T) - [\tau : \nabla v] + \left(\frac{\partial \ln V}{\partial \ln T}\right)_p v \cdot \nabla P + \rho T v \cdot \nabla c_p \tag{4}$$

Species balance equations, on the other hand, require knowledge of the dissociation pathways and related kinetic expressions for the gas mixture, SiH_4, N_2, and NH_3. Tsu et al. (1986) reported for a remote PECVD system for silicon nitride film growth that NH is the dominant reactive species in NH_3 glow discharges. Bardos et al. (1984) mentioned that SiH and SiN are the dominant reactive species in their system. Meanwhile, Nguyen et al. (1986) suggested the existence of SiH_x, NH_x, and N radicals. Typically, the reaction mechanisms associated with free radicals should include three steps: radical generation, propagation, and termination. The lack of kinetic data makes it meaningless to try to take all the steps into account. Instead, a representative dissociation scheme is assumed based on the previous studies as fol-

lows:

$$e^- + SiH_4 \rightarrow e^- + SiH + 3H$$
$$e^- + NH_3 \rightarrow e^- + NH + 2H$$
$$e^- + N_2 \rightarrow e^- + N + N$$

Therefore, the species balances can be written:

$$\nabla \cdot (\rho v \omega_i) = \nabla \cdot (\rho D_{im} \nabla \omega_i) + \theta_{ij} r_j \tag{5}$$

where i = SiH, NH, N, H, and r_j is the dissociation rate of the corresponding precursor gas for species i. The precursor gases are related to the four species above by reaction conversions. H radicals are generated by NH_3 and SiH_4 dissociations.

The system variables such as the individual gas flow rates and susceptor temperature come into the model through the boundary conditions, as do the surface reactions. For the momentum and energy equations, the boundary conditions are:

At the inlet

$$v = (0, v_{in})^T \tag{6}$$

$$T = T_{in} \tag{7}$$

At the outlet

$$(n \cdot \nabla v) = (0, 0)^T \tag{8}$$

$$(n \cdot \nabla T) = 0 \tag{9}$$

On solid surfaces

$$v = (0, 0)^T \tag{10}$$

$$(n \cdot \nabla T) = 0 \tag{11}$$

On the susceptor surface Eq. 11 is replaced by

$$T = T_s \tag{12}$$

In all the above n is the unit normal to the boundary under consideration, and i = SiH, NH, N, H.

For the species balance equations, boundary conditions were applied to the deposition region between the electrodes.

At the inlet to the deposition region:

$$\rho D_{im}(n \cdot \nabla \omega_i) = (n \cdot v)\rho \omega_i \tag{13}$$

At the outlet of the deposition region:

$$(n \cdot \nabla \omega_i) = 0 \tag{14}$$

On the substrates and reactor wall, it is assumed that the radicals react readily upon each collision; therefore, the deposition rate is equal to the collision rate evalulated from gas kinetic theory. On the other hand, hydrogen outdiffusion from the deposited film surface is a well-known phenomenon (Nguyen et al., 1986). To take into account the outdiffusion mechanism, it is assumed that SiH and NH release H with unit probability upon reacting on the film, and the H radicals react with a certain probability (γ) upon colliding on the substrate. The probability γ will be estimated by fitting the model to the experimental data. The boundary conditions on the solid surfaces are therefore

$$\rho D_{im}(n \cdot \nabla \omega_i) = \gamma \sqrt{\frac{RT}{2\pi M_i}} \rho \omega_i \tag{15}$$

where $\gamma = 1$ except in hydrogen.

Our experimental data show that only a small percentage of reactant gas is deposited. It is therefore further assumed, to be consistent with the assumption regarding deposition rate, that only a small fraction of precursor gas is dissociated, and the accompanying heat and volume changes are negligible. These assumptions enable decoupling of the species balance equations from the momentum and energy balance equations. The related physical properties such as heat capacity, viscosity, and thermal conductivity are taken as mixture averages evaluated with Chapman-Enskog theory and Wilke's semiempirical formula for the mixture (Bird et al., 1960). Related constants are found from the literature (Gordon and McBride, 1971; Svehla, 1962). To save computer time, mixture properties were evaluated at different temperatures and fitted to a simple polynomial, following Michaelidis and Pollard (1984). Based on the assumption of small percentage dissociation of precursor gases, the effective diffusivities, D_{im}, can be considered as the combination of the diffusion of radicals i in SiH_4, NH_3, and N_2. Calculations show that they are of the same order of magnitude; therefore, the average is taken as the diffusivity of species i in the mixture.

Dissociation Rate in a Glow Discharge

In a PECVD system the deposits are mainly formed through the condensation of free radicals that are generated from the electron impact dissociation of neutral molecules. The dissociation rate can be measured experimentally, and for some cases can be expressed by first-order kinetics (Nolet, 1975). The rate constants so obtained, however, are dependent on diluent gas and operating conditions. Therefore, the use of the rate constants can be very limited. Another way of formulating the dissociation rate is (Hollahan and Bell, 1974):

$$r_j = K_j N_e \rho \omega_j \tag{16}$$

that is, the rate is proportional to the product of the electron density and the precursor gas concentration. The rate constant, K_j, can then be determined from

$$K_j(\bar{\epsilon}) = \int_0^\infty \left(\frac{2\epsilon}{M_e}\right)^{1/2} \sigma_j(\epsilon) f(\epsilon, \bar{\epsilon})\, d\epsilon \tag{17}$$

The effects of operating conditions are resolved into two parameters, electron density N_e and mean electron energy $\bar{\epsilon}$. Obviously, in order to evaluate K_j the exact forms of the electron energy distribution function $f(\epsilon, \bar{\epsilon})$ and electron impact dissociation cross section $\sigma(\epsilon)$ need to be known.

The electron impact dissociation cross section can be measured experimentally (Perrin et al., 1982), but is often only available for a limited number of systems. Fortunately, data were available for the precursor gases used in this work. Published values were obtained and used for $\sigma(\epsilon)$ for SiH_4 (Perrin et

al., 1982), NH_3 (Slovetski and Urbas, 1979), and N_2 (Mamikonyan et al., 1972).

The electron energy distribution function $f(\epsilon, \bar{\epsilon})$ can be obtained from the solution of the Boltzmann equation (Hollahan and Bell, 1974; Reder and Brown, 1954). Although an exact solution does not appear to exist, Bell (1970) has presented some approximate solutions under the following assumptions:

1. Coulombic collisions are negligible
2. Energy loss through inelastic collisions is negligible

In the absence of the electrical field, a Maxwellian energy distribution results. With the presence of an oscillating electrical field, if one further assumes:

3. The energy gained from electrons colliding with faster moving molecules is much less than the energy gained from the electrical field
4. The electron collision frequency is much greater than the oscillating frequency of the electrical field

then if the momentum collision cross section is inversely proportional to electron velocity, a Margenau distribution is obtained. If the cross section is independent of the velocity, a Druyvesteyn distribution is found. The above assumptions are satisfied in prevailing glow discharge systems (Haller, 1983), except for that of negligible energy loss in inelastic collisions. Nevertheless, it has been shown that in the oxygen and methane glow discharge the electron energy distribution is Druyvesteynian (Myers, 1969; Tachibana et al., 1984). Rhee and Szekely (1986) used the Druyvesteyn distribution in their study of the PECVD of silicon. The distribution function is:

$$f(\epsilon, \bar{\epsilon}) = 1.04\bar{\epsilon}^{-3/2}\epsilon^{1/2} \exp\left[-0.55(\epsilon/\bar{\epsilon})^2\right] \tag{18}$$

where $\bar{\epsilon}$ is the mean electron energy, which is taken as uniform in the reactor.

The spatial distribution function for electron density N_e can be determined theoretically provided the related parameters are available. Graves and Jensen (1986) solved a quite detailed continuum model for RF and DC discharges, and concluded that "the ambipolar diffusion model is a promising way to simplify predictions of discharge physics." Both the ambipolar diffusion model (Dalvie et al., 1986) and a simple polynomial distribution function (Chen, 1983) have previously been used for reactor modeling. Although the ambipolar model does not properly represent the distribution of electrons in the sheath region, its simple form is a convenient approximation that helps keep the model equations tractable.

The electron density is hypothesized to be uniform in the radial direction, but distributed across the electrode spacing according to the ambipolar diffusion model:

$$N_e = N_{e0} \cos\left\{[(z - z_0)/H - \tfrac{1}{2}]\pi\right\} \tag{19}$$

where N_{e0} is the density at the reactor center. According to Bell (1970), this can be expressed as:

$$N_{e0} = K_e T\langle P\rangle/P \tag{20}$$

where K_e is a constant if the system pressure and temperature are uniform. In this case the mean electron density can be found by integrating Eq. 19 to give

$$\overline{N}_e = (2/\pi)K_e T\langle P\rangle/P \tag{21}$$

An estimate of the electron impact dissociation rate of a precursor gas in a PECVD system is possible provided the electron density, electron energy distribution function, and impact dissociation cross section are known. The simplified models for these quantities presented above are necessary to keep the reactor model tractable. Equation 17 can be integrated numerically to obtain the dissociation rate constants K_j as functions of mean electron energy, as shown in Figure 2. It is seen that for a mean electron energy between 3 and 7 eV, the dissociation rates of NH_3 and SiH_4 are close, and the rate of N_2 is an order of magnitude smaller. This is the region of most interest for a RF glow discharge plasma.

Model Solution and Simulations

Equations 2 to 20 form the model for the current PECVD process with K_e (electron density constant), $\bar{\epsilon}$ (mean electron energy), and γ (the hydrogen reaction probability) being the adjustable parameters. The model equations were solved by the finite-element method, using the PDE/PROTRAN package (Sewell, 1985; Mills and Ramachandran, 1988). The solutions were considered acceptable only if two convergence criteria were satisfied:

1. With a fixed number of elements, the solution changed within the tolerance for two successive iterations
2. The converged solutions was further tested by increasing the number of elements, until it converted with respect to number of elements used

Converged solutions to the Navier-Stokes and energy equations were found with 430 quadratic elements. It was found that parameterization significantly improved the convergence. This was done by multiplying the convective terms of the momentum and energy balance equations by a parameter. The parameter value progressively increases with the number of iterations from zero to one; once the value reaches one it stays constant until the

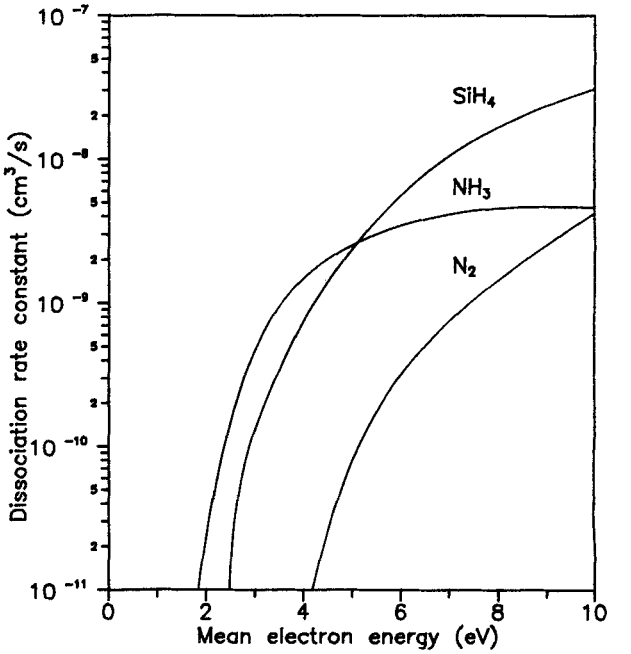

Figure 2. Mean electron energy dependence of electron impact dissociation rate constants.

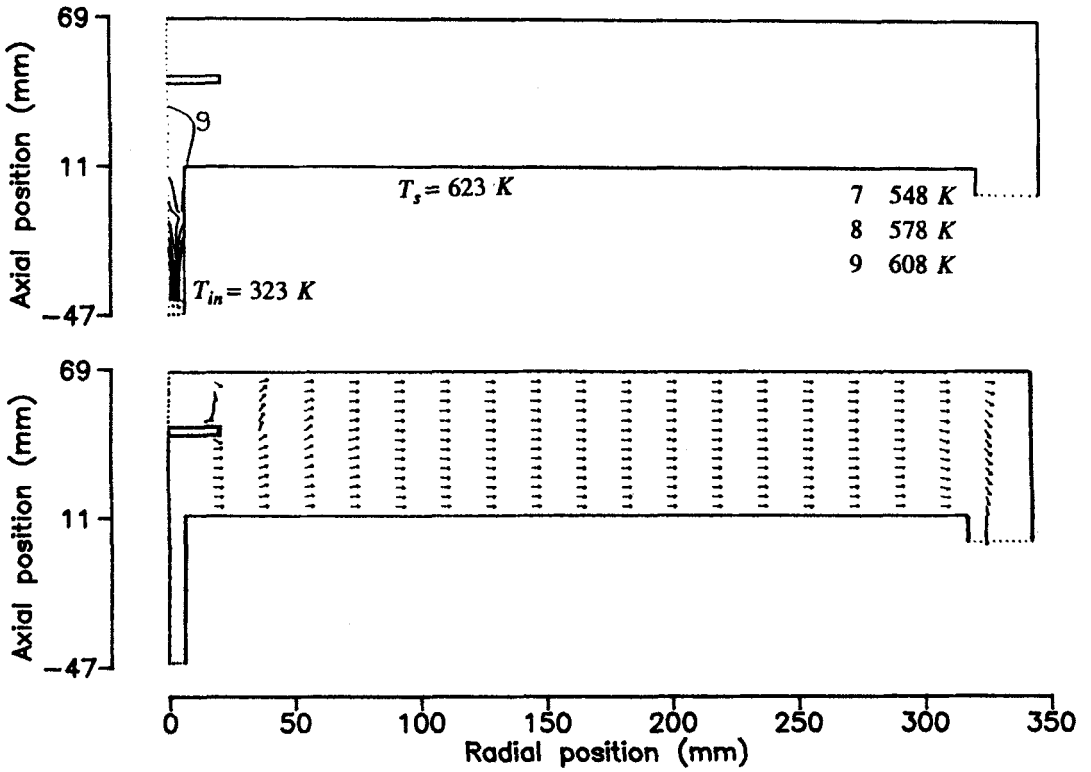

Figure 3. Temperature and velocity profiles in PECVD reactor.

solution converges. In other words, one starts to solve the set of nonlinear PDE's by solving its pseudolinear counterpart.

A typical flow pattern, shown in Figure 3, shows no circulation except at the edge of the gas shield. It also shows that the inlet gas is heated to near the susceptor temperature at the entrance of the deposition zone; the deposition zone can very well be considered isothermal.

The species balance equations were solved within the electrode region; the converged solutions were found with 50 quartic elements. Under typical operating conditions, the equations were solved with various values of mean electron energy and electron density constant. Figure 4 shows the effects of the mean electron energy and electron density constant on the film deposition rates and Si/N ratios. The mean electron density is proportional to the electron density constant. It can be seen that the model predicts that growth rates increase with both mean electron density and energy, while the film composition only varies with mean electron energy. The case here is like a simple parallel reaction, A reacting to form B and C. An increase in the concentration of A raises the reaction rate, but does not affect the selectivity. Changes in temperature would alter both the reaction rate and selectivity, provided the activation energies are different.

Comparison of Model to Data

Table 1 shows base case operating conditions of the PECVD system. The experimental data corresponding to the base case conditions are shown in Figure 5. Growth rate was calculated directly from measured weight gain. All data points were repeated and show good reproducibility. The film growth rates and compositions were uniform along the susceptor radius, except for slighly lower rates near the inlet region.

Figure 5 shows that the model predictions agree with the experimental data for both film growth rates and compositions. The hydrogen reaction probability on the substrate surface was $\gamma = 2.2 \times 10^{-4}$, which was used for all the model predictions at the same susceptor temperature as the base case. The mean electron density, $\bar{N}_e$, was found to be 2.37×10^{14} cm^{-3} and the mean electron energy, $\bar{\epsilon}$, was 6.98 eV. The mean electron energy and density found are comparable to literature values. According to

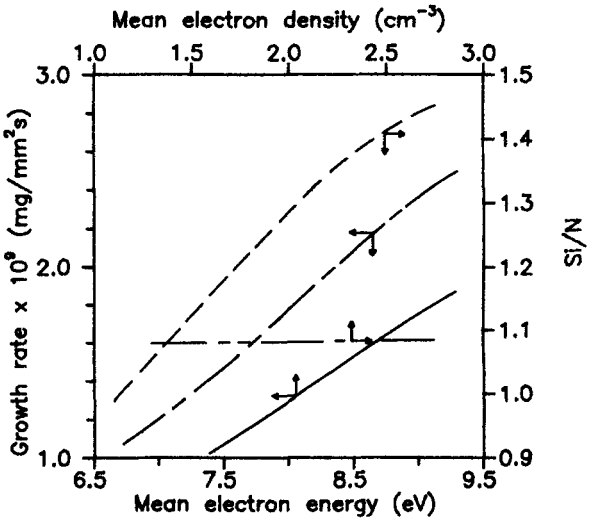

Figure 4. Effect of mean electron density and energy on film growth rates and compositions.

Table 1. Base Case Operating Conditions of the PECVD System

Operating Variables	Settings
Power input	500 W
Pressure	1.5×10^{-3} N/m^2
Flow rate	1,600 cm^3/s (STP)
Temperature	350°C
$SiH_4/NH_3/N_2$	1/1.69/1.69

Hollahan and Bell (1974), the mean electron energy is in the range 1–10 eV. Electron density has been experimentally measured in parallel plate reactors for different gas systems. The electron density was about 10^{15} cm^{-3} in the system of DeVries et al. (1985) under 3.75×10^{-4} N/m^2 (0.05 torr) and power density of 0.3 W/cm^2. The density was of order 10^9 cm^{-3} in the system of Allen et al. (1986) under 3.75×10^{-3} N/m^2 (0.5 torr) and power density of 0.4 W/cm^2. The current system typically operated at 1.5×10^{-3} N/m^2 (0.2 torr) and power density of 0.16 W/cm^2.

In an earlier study of this system (Yoo and Dixon, 1989), it was found that over the range of operating parameters the Si/N ratio was mainly affected by reactant gas composition and, to a lesser extent, system pressure. The film growth rate was mainly affected by power level and, again to a lesser extent, temperature and pressure. These results were confirmed by the data in the present study.

It has been observed that the mean electron energy at gas breakdown is a function of gas composition (Van Burt, 1987). Therefore, it is possible that both K_e and mean electron energy would vary as gas composition changes. The model-fitting in Figure 6 shows that increases in silane mole fraction lead to a slight increase in estimated mean electron density and a slight decrease in estimated mean electron energy.

Temperature affected growth rate only to a small extent. As temperature decreased from 350 to 50°C the estimated $\bar{N}_e$ decreased from 2.37×10^{14} to 1.60×10^{14} cm^{-3} and the γ increased from 2.2×10^{-4} to 2.8×10^{-4}. These effects may offset so that little effect of temperature is observed.

From the above discussion, it can be seen that by adjusting the parameter values the model fits the experimental film growth rates and compositions well for various reaction conditions. A predictive model for the effects of changes in operating variables is much harder to obtain, as in most cases it is not yet known how the mean electron energies and densities depend on the system conditions.

Predictive Nature of the Model

A test of the predictive power of the model is obtained by using the parameters evaluated at a power input of 500 W to predict the film compositions and deposition rates at other power input levels. The electron density constant K_e is not power-input dependent; neither is the hydrogen reaction probability γ. Yoo and Dixon (1989) showed that the power input does not affect the film Si/N ratio. Since the film Si/N ratio is a strong func-

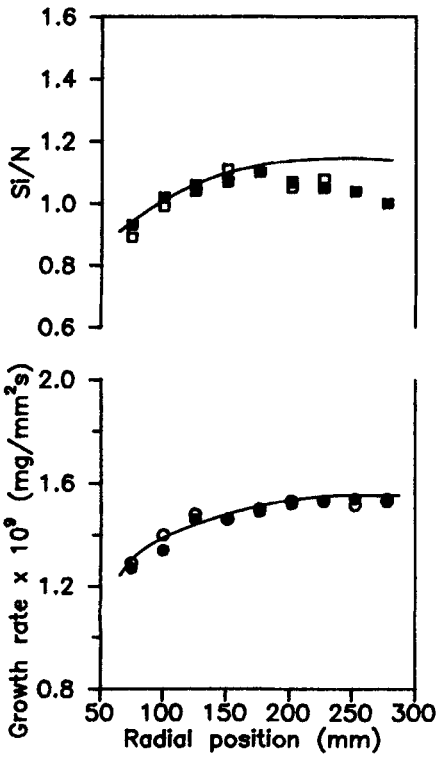

Figure 5. Experimental film compositions and growth rates v. model predictions for base case conditions.
$\bar{N}_e = 2.37 \times 10^{14}$ cm^{-3}; $\bar{\varepsilon} = 6.98$ eV

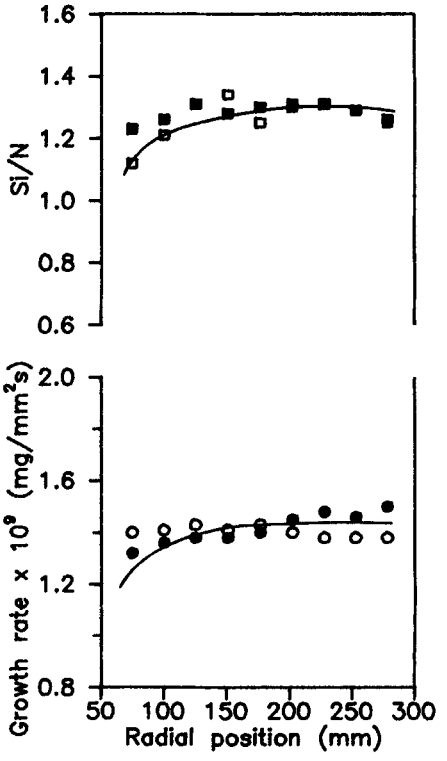

Figure 6. Experimental film compositions and growth rates v. model predictions for a $SiH_4/NH_3/N_2$ ratio of 1/1/1.26.
$\bar{N}_e = 3.0 \times 10^{14}$ cm^{-3}; $\bar{\varepsilon} = 6.45$ eV

tion of mean electron energy, as shown in Figure 4, the mean electron energy must stay constant as power input changes. This implies that the three parameters do not vary with the system power input. Therefore, according to Eq. 20, the effect of an increase in power is to increase the electron density. This has been observed experimentally (Allen et al., 1986; Tachibana, 1984). Figure 7 shows that the model correctly predicts the trend of the growth rate changes with power input, and the model predictions are within 10% deviation from the experimental data.

The observed small but systematic deviation between the model predictions and the experimental data can be explained by noting that the electrons can diffuse out of the electrode region in the current system, resulting in a reduced effective power input, as observed by Dun et al. (1981) and Reinberg (1979). The outgrowth of the plasma is more serious at high power levels than at low power. If the constant K_e is estimated at a medium to high power input level, so that the value of the constant reflects a mild extent of plasma outgrowth, and then is used to predict deposition rates at other power levels, the model predictions will overestimate the deposition rates at high power levels because the effective power input (the actual power that causes the deposition) is smaller than the nominal power input (the power that is used in the model and is the setting of the reactor) due to the plasma outgrowth. Conversely, this reasoning explains why the model predictions underestimate the deposition rate experimental data at low power levels where plasma outgrowth is less serious.

The extent of plasma outgrowth increases with the power input; that is, the difference between the effective power input and the nominal power input is larger at higher power levels. Hence it can be assumed that the effective power input is $\langle P \rangle^x$ and x is less than unity. For the current case, if one uses $x = 0.8$, the model predictions fall much closer to the experimental data, as shown in Figure 8. The value of x is related to the plasma outgrowth. If shielding can perfectly avoid the outgrowth then x equals one; x is close to zero if there is a serious plasma outgrowth, for example if the bell jar or process chamber is much larger than the electrode region.

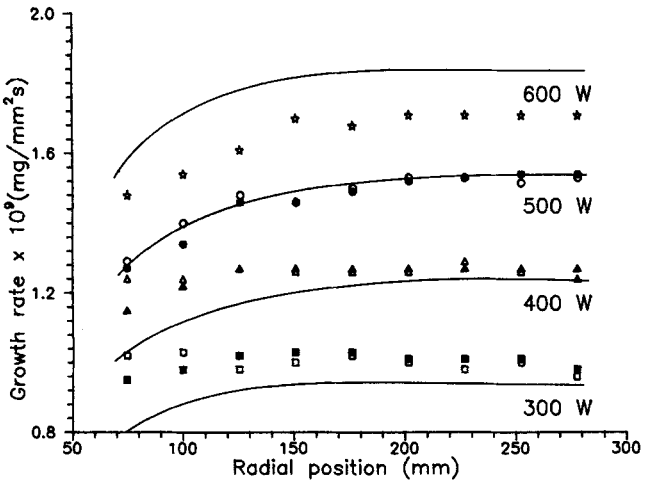

Figure 7. Model predictions v. experimental data for film growth at various power levels.
$\bar{N}_e = 2.37 \times 10^{14}\ \text{cm}^{-3}$; $\bar{\epsilon} = 6.98$ eV

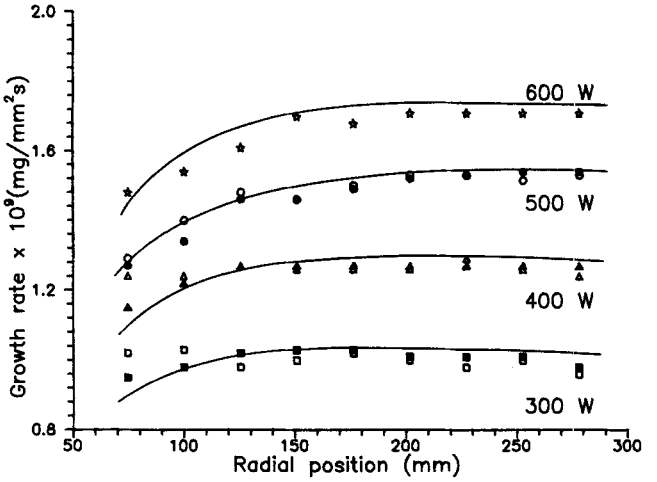

Figure 8. Model predictions with effective power inputs.
Electron density $\alpha\ \langle P \rangle^{0.8}$; $\bar{N}_e = 2.37 \times 10^{14}\ \text{cm}^{-3}$; $\bar{\epsilon} = 6.98$ eV

Conclusions

This study has experimentally investigated the effects of operating variables on film compositions and growth rates for PECVD of Si-N-H films grown from a gas mixture of SiH_4, NH_3, and N_2. The film compositions and growth rates are well correlated to reactor operating conditions with a nonisothermal PECVD reactor model taking into account the temperature dependence of physical properties. The experimental data show good reproducibility at various conditions. The model solution shows that the deposition zone can be considered isothermal. For various reactor operating conditions the model solutions for film compositions and growth rates fit the experimental data well by adjusting the mean electron density and energy. The model is partially predictive, correctly predicting film compositions and growth rates for various power levels.

Acknowledgment

The authors thank Sprague Electric I.C. Division, Worcester, MA, for providing all the experimental facilities. Help from John MacDougall and the engineering group, Clarke Andersen, Wayne Roberson, Kelly Vinner, and Tony Lavana, is highly appreciated. C-S. Yoo was supported by a Chang Fellowship from the Department of Chemical Engineering, Worcester Polytechnic Institute, during this research.

Notation

A = Avogadro's number
c_p = specific heat of gas mixture
D_{im} = effective diffusivity of species i in gas mixture
$f(\epsilon, \bar{\epsilon})$ = electron energy distribution function
g = gravity vector
H = electrode spacing
K = thermal conductivity of gas mixture
K_e = electron density constant
K_j = dissociation rate constant of species j
M = average molecular weight of a film
M_i = molecular weight of species i
M_e = mass of electron
n = film refractive index
n = unit normal to a boundary surface
N_e = electron density
N_{e0} = electron density at reactor center
P = system pressure
$\langle P \rangle$ = power input

r_j = dissociation rate of precursor species j
R = gas constant
T = system temperature
T_{in} = temperature of inlet gas
V = specific volume
v = velocity vector
v_{in} = velocity of inlet gas
z = height from bottom electrode
z_0 = height of bottom electrode

Greek letters

α_i = apparent electronic polarizability of species i
α_e = average electronic polarizability
ϵ = electron energy
$\bar{\epsilon}$ = mean electron energy
ρ = gas density
ω_i = mass fraction of species i
σ_j = electron impact dissociation cross section of species j
θ_{ij} = product of stoichiometric coefficient and molecular weight ratio of a radical i to its precursor gas j
τ = viscious stress tensor
γ = hydrogen reaction probability

Literature Cited

Allen, K. D., H. Sawin, M. Mocella, and M. W. Jenkins. "The Plasma Etching of Polysilicon with CF_3Cl/Argon Discharge," *J. Electrochem. Soc.*, **133,** 2315 (1986).

Bardos, L., J. Musil, and M. Lubanski, "Chemiluminescence of the Silane-Active Nitrogen Reaction During PECVD of the Silicon Nitride Films," *Czech. J. Phys.*, **B34,** 1242 (1984).

Bell, A. T., "Spatial Distribution of Electron Density and Electrical Field Strength in a High-Frequency Discharge," *Ind. Eng. Chem. Fundam.*, **160** (1970).

Bird, R. B., W. E. Stewart, and E. N. Lightfoot, *Transport Phenomena,* Wiley, New York (1960).

Bohn, P. W., and R. C. Manz, "A Multiresponse Factorial Study of Reactor Parameters in Plasma-Enhanced CVD Growth of Amorphous Silicon Nitride," *J. Electrochem. Soc.*, **132,** 1981 (1985).

Chen, I., "Mass Transfer Analyses of the Plasma Deposition Process," *Thin Solid Films,* **101,** 41 (1983).

Dalvie, M., K. F. Jensen, and D. Graves, "Modeling of Reactor for Plasma Processing. I: Silicon Etching by CF_4 in a Radial-Flow Reactor," *Chem Eng Sci.*, **41,** 653 (1986).

deVries, C. A. M., A. J. van Roosmalen, and G. C. C. Puylaert, "Microwave Spectroscopic Measurement of the Electron Density in a Planar Discharge: Relation to Reactive Ion Etching of Silicon Oxide," *J. Appl. Phys.*, **9,** 4386 (1985).

Dun, H., P. Pan, F. R. White, and R. W. Douse, "Mechanism of Plasma-Enhanced Silicon Nitride Deposition Using SiH_4/N_2 Mixture," *J. Electrochem. Soc.*, **128,** 1555 (1981).

Gordon S., and B. J. McBride, "Computer Program for Calculation of Complex Chemical Equilibria, Rocket Performance, Incident and Reflected Shocks, Chapman-Jouquet Detonations," NASA SP-273 (1971).

Graves D. B., and K. F. Jensen, "A Continuum Model of DC and RF Discharges," *IEEE Trans. Plasma Science,* **14,** 78 (1986).

Haller, I., "Importance of Chain Reactions in the Plasma Deposition of Hydrogenated Amorphous Silicon," *J. Vac. Sci. Technol.*, **A1,** 1376 (1983).

Hill, N. E., W. E. Vaughan, A. H. Price, and M. Davies, *Dielectric Properties and Molecular Behavior,* Van Nostrand Reinhold, London (1969).

Hollahan, J. R., and A. T. Bell, *Technique and Application of Plasma Chemistry,* Wiley, New York (1974).

Kember, P. N., S. C. Liddell, and P. Blackborrow, "Characterizing Plasma-Deposited Silicon Nitride," *Semiconduc. Inter.*, **8,** 158 (1985).

Lanford, W. A., and M. J. Rand, "The Hydrogen Content of Plasma-Deposited Silicon Nitride," *J. Appl. Phys.*, **49,** 2473 (1978).

Mamikonyan, E. R., L. S. Polak, and D. I. Slovetskii, "Dissociation of Nitrogen Molecules from Electrically Excited States (Electron Impact Dissociation)," *Khim. Vys. Energ.*, **6,** 483 (1972).

Michaelidis, M., and R. Pollard, "Analysis of Chemical Vapor Deposition of Boron," *J. Electrochem. Soc.*, **131,** 860 (1984).

Mills, P. L., and P. A. Ramachandran, "Mathematical Modeling of Chemical Engineering Systems by Finite-Element Analysis Using PDE/PROTRAN," *Comput. Math. Applic.*, **15,** 769 (1988).

Mort, J., and F. Jansen, *Plasma-Deposited Thin Films,* CRC Press, Boca Raton, FL (1985).

Myers, H., "Analysis of Electron Swarm Experiments in Oxygen," *J. Phys.*, **B2,** 393 (1969).

Nguyen, V. W., S. Burton, and P. Pan, "The Variation of Physical properties of Plasma-Deposited Silicon Nitride and Oxynitride with Their Compositions," *J. Electrochem. Soc.*, **131,** 2348 (1984).

Nguyen, V. S., S. Burton, and P. Pan, "The Variation of Physical propgen Bonding, Depth Profiles, and Spin Density in Plasma-Deposited Silicon Nitride and Oxynitride with Deposition Mechanism," *J. Electrochem. Soc.*, **133,** 970 (1986).

Nolet, G., "Kinetics of Decomposition of Silane (Diluted in Argon) in a Low-Pressure Glow Discharge," *J. Electrochem. Soc.*, **122,** 1030 (1975).

Perrin, J., J. P. M. Schmidt, G. deRosney, B. Oevillan, and A. Lioret, "Dissociation Cross Section of Silane by Electron Impact," *Chem. Phys.*, **73,** 393 (1982).

Reder F. H., and S. C. Brown, "Energy Distribution Function of Electrons in Pure Helium," *Phys. Rev.*, **95,** 885 (1954).

Reinberg, A. R., "Plasma Deposition of Inorganic Silicon Containing Films," *J. Electronic Material,* **8,** 345 (1979).

Rhee, S., and J. Szekely, "The Analysis of Plasma-Enhanced Chemical Vapor Deposition of Silicon Films," *J. Electrochem. Soc.*, **133,** 2194 (1986).

Rosler, R. S., W. C. Benzing, and J. Baldo, "A Production Reactor for Low-Temperature Plasma-Enhanced Silicon Nitride Deposition," *Solid State Technol.*, **6,** 45 (1976).

Samuelson, G. M., and K. M. Mar, "The Correlations Between Physical and Electrical Properties of PECVD Si-N with Their Composition Ratios," *J. Electrochem. Soc.*, **129,** 1773 (1982).

Sewell, G., *Analysis of a Finite Element Method: PDE/PROTRAN,* Springer, Berlin (1985).

Sinha, A. K., and E. Lugujjo, "Lorentz-Lorenz Correlation for Reactive Plasma Deposited Si-N Films," *Appl. Phys. Lett.*, **32,** 245 (1978).

Slovetskii, D. I., and A. D. Urbas, "Cross Section for the Dissociation of Ammonia by Electron Impact," *Khim. Vys. Energ.*, **13,** 475 (1979).

Sterling, H. F., and R. C. G. Swann, "Chemical Vapor Deposition Promoted by RF Discharge," *Solid State Electronics,* **8,** 653 (1965).

Svehla, R. A., "Estimated Viscosities and Thermal Conductivities of Gases at High Temperatures," NASA TR R-132 (1962).

Tachibana, K., H. Todokoro, H. Harima, and Y. Urono, "Diffusion of Silicon Atoms and Their Film Deposition in a Silane-Argon Plasma," *J. Phys.*, **D15,** 177 (1984).

Tsu, D. V., G. Lucovsky, and M. J. Mantini, "Local Atomic Structure in Thin Films of Silicon Nitride and Silicon Diimide Produced by Remote Plasma-Enhanced CVD." *Phys., Rev.*, **B33,** 7096 (1986).

Van Burt, R. J., "Common Parameterizations of Electron Transport, Collision Cross Section, and Dielectric Strength Data for Binary Gas Mixtures," *J. Appl. Phys.*, **61,** 1773 (1987).

Yoo, C-S., and A. G. Dixon, "Factorial Experimental Investigation of PECVD of Silicon Nitride Thin Films," *Thin Solid Films,* **168** 281 (1989).

Manuscript received May 9, 1988, and revision received Jan. 20, 1989.